2014 IEEE International Conference on Robotics & Automation (ICRA)
Hong Kong Convention and Exhibition Center
May 31 - June 7, 2014. Hong Kong, China

Human-Guided Robotic Manipulation: Theory and Experiments

X. Li and C. C. Cheah

***Abstract*— Emerging applications of robot systems that involve close physical interaction with human have opened up new challenges in robot control. For these applications, it is important to consider the stability and coordination of human-robot interaction. While various control techniques have been developed for human-robot interaction, existing methods do not take the advantages of human ability in responding and adapting to unknown environment. In this paper, a human-guided manipulation problem which is able to take advantages of both the human knowledge and the robot's ability, is formulated and solved. The workspace is divided into a human region, where human play a more active role in the manipulation task, and a robot region, where the robot is more dominant in the manipulation. The proposed formulation allows the involvement of human control action to deal with unforeseen changes or uncertainty in the real world. We present a theoretical foundation that allows the stability and coordination of the human-guided manipulation problem to be analyzed. Based on the human region and the robot region, an adaptive tracking controller is developed. Experimental results are presented to illustrate the performance of the proposed control method.**

I. INTRODUCTION

Rapid advances in robotic technologies have led to the emergence of a diversity of initiatives that involves physical interactions with human, such as rehabilitation robots [1]–[3] and exoskeleton or wearable robots [4], [5]. The rehabilitation robots are developed to help stroke patients to restore the impaired functionalities of limbs, and the wearable robots are used to enhance the strength or complement the ability of human. The development of human-robot interaction systems widens the potential applications of traditional robot manipulators and also creates systems that are beyond the physical capability of human body.

Though much progress has been achieved in understanding motion control of robot manipulator [6]–[13], most results are limited to the case of isolated robot systems that do not involve physical interactions with human. By using Lyapunov method, Takegaki and Arimoto [6] showed that a simple PD controller with gravity compensation was effective for setpoint control, despite the nonlinearity of robot dynamics. To deal with trajectory tracking control with parametric uncertainty, several adaptive control schemes [7], [8] were proposed for robot manipulator. Various task-space sensory controllers have also been proposed for robotic manipulator with uncertainties in both kinematics and dynamics [9]–[11]. In addition, the concept of task-space region control was proposed in [12], where the desired objective can be specified as a region, instead of a desired position or trajectory. Recently, a new task-space control method using regional feedback information was also proposed in [13] such that the global dynamic stability with the consideration of singularity issues and limited sensing zones was guaranteed.

For applications that involve close interaction and cooperation with human, several works have been reported in the literature to address the issues of safety and performance in physical human-robot interaction, such as the use of lightweight robots [14], passive compliant systems [15], and variable stiffness actuation (VSA) [16], [17]. Bicchi and Tonietti [18] considered the problem of designing joint-actuation mechanisms, which not only guarantees low injury risk but also allows the fast and accurate operation of the robot. In [19], a non-model based method with less predictable interactions between patients and devices was developed for rehabilitative systems. To handle the reaction of robotic system to environmental forces, a novel concept of impedance control was firstly brought up by Hogan *et al.* [20], [21] and is now commonly used in tasks involving physical human-robot interaction. In impedance control, the desired performance of human-robot interaction is specified by a desired impedance between the motion of robot and the forces of interaction. By specifying the performance of robot system with a target impedance, an iterative learning impedance controller was proposed in [22]. An impedance-based control algorithm was developed in [23], for ankle rehabilitation using parallel robot. In [24], an active impedance controller was proposed to increase the Cartesian stiffness range of VSA. An adaptive impedance scheme was developed in [25] to compensate unmodeled uncertainty in a collaborative task that requires sharing of a load by two partners. In [26], an adaptive controller was presented for upper-limb rehabilitative robotic systems, where a position-dependant stiffness was introduced to resolve the possible conflicts between patients and robots.

However, existing control techniques for human-robot interaction do not provide much flexibility for cooperative manipulation tasks that require human's guidance and assistance, and the advantages of human ability in responding and adapting to unknown environment are not fully explored or utilized in the control method. It is interesting to observe that humans are able to react intelligently to unforeseen changes in the real world and perform skillful manipulation tasks. Industrial robot manipulators, on the contrary, are designed to operate in a structured environment and is able to carry heavy loads that are beyond the capability of human.

In this paper, we formulate a human guided manipulation problem that is able to take advantages of both the human

The authors are with the School of Electrical and Electronic Engineering, Nanyang Technological University, Singapore, 639798. The work was supported by the Agency For Science, Technology And Research of Singapore (A*STAR), (reference 1225100002).

knowledge and the robot's ability in a stable manner. We present a theoretical foundation that allows the analysis of the human-guided manipulation problem. To formulate the co-manipulation tasks, the workspace is divided into a human region, where human plays a more active role in the manipulation task, and a robot region, where the robot is more dominant in the manipulation. The human region allows the involvement of human control action to take advantages of human knowledge for manipulation in an unknown environment, while the robot region allows the robot to take control in cases when manipulation task is well defined. Based on these regions, an adaptive tracking controller is developed so as to take the advantages of both the human knowledge and the ability of robot. It is shown that the stability of closed-loop system is guaranteed. Experimental results are presented to illustrate the performance of the proposed control method.

II. Robot Kinematics and Dynamics

Let $\boldsymbol{x}$ denotes the position of the end effector in task space [9], such as Cartesian space or image space. If $\boldsymbol{x}$ is specified in Cartesian space, we have $\boldsymbol{x}=\boldsymbol{r}\in\Re^{n_r}$ which is the position of the end effector in Cartesian space. If $\boldsymbol{x}$ is specified in image space, we have $\boldsymbol{x}=\boldsymbol{x}_I\in\Re^2$ which is the position of image feature. The Cartesian-space velocity of the end effector $\dot{\boldsymbol{r}}$ is related to the joint-space velocity $\dot{\boldsymbol{q}}$ as [27]:

$$\dot{\boldsymbol{r}}=\boldsymbol{J}_r(\boldsymbol{q})\dot{\boldsymbol{q}}, \tag{1}$$

where $\boldsymbol{q}\in\Re^n$ is the vector of joint variables, and $\boldsymbol{J}_r(\boldsymbol{q})$ is the Jacobian matrix from joint space to Cartesian space. The image velocity vector $\dot{\boldsymbol{x}}$ is related to the Cartesian-space velocity and the joint-space velocity as [11], [13]:

$$\dot{\boldsymbol{x}}_I=\boldsymbol{J}_I(\boldsymbol{r})\dot{\boldsymbol{r}}=\boldsymbol{J}_I(\boldsymbol{r})\boldsymbol{J}_r(\boldsymbol{q})\dot{\boldsymbol{q}}=\boldsymbol{J}(\boldsymbol{q})\dot{\boldsymbol{q}}, \tag{2}$$

where $\boldsymbol{J}_I(\boldsymbol{r})$ is the interaction matrix or image Jacobian matrix, and $\boldsymbol{J}(\boldsymbol{q})=\boldsymbol{J}_I(\boldsymbol{q})\boldsymbol{J}_r(\boldsymbol{q})\in\Re^{2\times n}$ is the Jacobian matrix of the mapping from joint space to image space.

When the robotic manipulator interacts with human, the dynamic model of robot is described as:

$$\boldsymbol{M}(\boldsymbol{q})\ddot{\boldsymbol{q}}+[\tfrac{1}{2}\dot{\boldsymbol{M}}(\boldsymbol{q})+\boldsymbol{S}(\boldsymbol{q},\dot{\boldsymbol{q}})]\dot{\boldsymbol{q}}+\boldsymbol{g}(\boldsymbol{q})+\boldsymbol{d}=\boldsymbol{\tau}+\boldsymbol{\tau}_e, \tag{3}$$

where $\boldsymbol{M}(\boldsymbol{q})$ is an inertia matrix which is symmetric and positive definite, $\boldsymbol{S}(\boldsymbol{q},\dot{\boldsymbol{q}})$ is a skew-symmetric matrix, $\boldsymbol{g}(\boldsymbol{q})$ denotes a vector of gravitational force, $\boldsymbol{d}$ is a unmodeled torque, $\boldsymbol{\tau}$ denotes a vector of control inputs, and $\boldsymbol{\tau}_e$ denotes the torque exerted on the robot by the human. If an external force $\boldsymbol{f}_e$ is exerted on the end effector, then $\boldsymbol{\tau}_e=\boldsymbol{J}^T(\boldsymbol{q})\boldsymbol{f}_e$. The dynamic model described by equation (3) is linear in a set of parameters $\boldsymbol{\theta}_d=[\theta_{d1},\cdots,\theta_{dn_d}]^T$ as [27], [28]: $\boldsymbol{M}(\boldsymbol{q})\ddot{\boldsymbol{q}}+[\frac{1}{2}\dot{\boldsymbol{M}}(\boldsymbol{q})+\boldsymbol{S}(\boldsymbol{q},\dot{\boldsymbol{q}})]\dot{\boldsymbol{q}}+\boldsymbol{g}(\boldsymbol{q})=\boldsymbol{Y}_d(\boldsymbol{q},\dot{\boldsymbol{q}},\dot{\boldsymbol{q}},\ddot{\boldsymbol{q}})\boldsymbol{\theta}_d$, where $\boldsymbol{Y}_d(\boldsymbol{q},\dot{\boldsymbol{q}},\dot{\boldsymbol{q}},\ddot{\boldsymbol{q}})\in\Re^{n\times n_d}$ is a dynamic regressor.

III. Human Region and Robot Region

Since human is able to react intelligently to unforeseen changes in the real world while robot is able to carry heavy loads that are beyond the capability of human, the human-robot co-manipulation can take advantage of both the human knowledge and the robot's ability. In this section, a theoretical foundation is presented for the analysis of the human-robot co-manipulation problem. To formulate the co-manipulation tasks, the workspace is divided into a human region, where human play a more active role in the manipulation task, and a robot region, where the robot is more dominant in the manipulation.

A. Scenarios of Human-Robot Co-manipulation

Based on the human region and robot region, we consider two scenarios of the co-manipulation task, where human play an active role in the beginning of the task and the robot only takes the control in the end, or the robot is active in the beginning and human guide the robot to carry out manipulation tasks in the end.

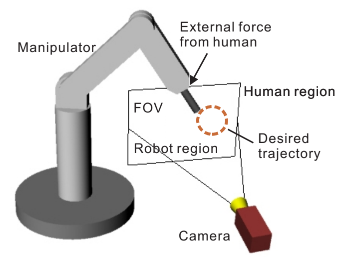

Fig. 1. The human region is specified outside the view of camera while the robot region is specified within the view. Human guide the end effector to enter the robot region and then the robot takes the control to drive the end effector to the desired position with visual feedback.

The first scenario is illustrated in Fig. 1. In Fig. 1, a camera is employed to measure the position of the end effector in image space, and the end effector is controlled to move to a desired position with visual feedback. However, due to limited field of view (FOV) of the camera, the robot does not have any visual information of the environment that is not within the view. The unknown environment of the robot workspace that is outside the view of the camera is thus defined as the human region. Human are expected to take control first and guide the end effector through the unknown environment towards robot region that is within the view of the camera. After the end effector enters the robot region, human can reduce or release the control and the robot then plays a more active role and drives the end effector to the desired position. In this scenario, the path of the end effector in the beginning is unknown or the environment is uncertain.

The second scenario is illustrated in Fig. 2, where the ending stage of the task is uncertain or unknown. In a complex environment with cluttered background, it is difficult to identify the desired position of the target and the positions of the obstacles in the workspace by using sensors such as vision systems. The positions of the target and obstacles are therefore unknown or uncertain. The uncertain environment of the workspace is therefore defined as the human region, and the region where the robot has the exact knowledge about the environment is defined as the robot region. The robot takes control first and drives the end effector from the robot region to the human region. After the end effector enters the human region, the robot becomes passive, and human identify the desired position and obstacles and guide the end effector to move to the desired position. In this scenario, the path of the end effector in the ending stage is unknown or the desired position and obstacles are uncertain.

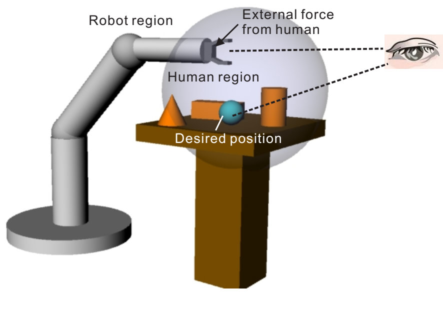

Fig. 2. It is difficult to identify the desired position due to the obstacles around it. Human identify the desired position and guide the end effector such that the position of the end effector converges to the desired position.

B. Region Function and Potential Energy

As seen from the previous subsection, the human region and the robot region should be specified such that human or the robot only takes control within the corresponding region, which allows the involvement of a more active control action when the other becomes passive. The region function of the human region and the robot human is specified as:

$$f(\boldsymbol{x})=\frac{(x_1-x_{d1})^{n_x}}{(x_{b1}-x_{d1})^{n_x}}+\cdots+\frac{(x_p-x_{dp})^{n_x}}{(x_{bp}-x_{dp})^{n_x}}-1\leq 0, \tag{4}$$

where $\boldsymbol{x}\in\Re^p$ is the position of the end effector in task space, the vector $\boldsymbol{x}_d=[\boldsymbol{x}_{d1},\cdots,\boldsymbol{x}_{dp}]^T$ denotes the desired position, $\boldsymbol{x}_b=[\boldsymbol{x}_{b1},\cdots,\boldsymbol{x}_{bp}]^T$ represents the bound of the region, and n_x is the order. The region function in equation (4) can be specified as a circle, an oval, or a rectangle with rounded corners by varying the order n_x, for different robot tasks. The regions where $f(\boldsymbol{x})\leq 0$ and $f(\boldsymbol{x})>0$ correspond to the human region and the robot region separately, which can also be opposite depending on the specific scenario. Next, the potential energy for the region function is to be developed.

1) : Consider the first scenario in the previous section, the human region is specified where $f(\boldsymbol{x})>0$ while the robot region is specified where $f(\boldsymbol{x})\leq 0$. Therefore, the potential energy is specified as:

$$P_t(\boldsymbol{x})=\frac{k_t}{N}\{1-[min(0,f(\boldsymbol{x}))]^N\}, \tag{5}$$

where k_t is a positive constant, $N\geq 4$ is an even integer, and the order of the region function in equation (4) is $n_x=2$. The bottom point of $P_t(\boldsymbol{x})$ corresponds to the desired position, but the top contour of $P_t(\boldsymbol{x})$ is varying as the desired position $\boldsymbol{x}_d$ is time-varying, which cannot match the fixed robot region and human region. To solve the problem, another potential energy function with a high-order reference region is introduced as:

$$P_h(\boldsymbol{x})=\frac{k_h}{N^2}\{min[0,[min(0,f_h(\boldsymbol{x}))]^N-(\kappa_h^{n_h}-1)^N]\}^N, \tag{6}$$

where $f_h(\boldsymbol{x})$ is the high-order reference region specified as: $f_h(\boldsymbol{x})=\frac{(x_1-x_{d1})^{n_h}}{(x_{b1}-x_{d1})^{n_h}}+\cdots+\frac{(x_p-x_{dp})^{n_h}}{(x_{bp}-x_{dp})^{n_h}}-1\leq 0$, and n_h is the order of the function, k_h is a positive constant, and $0<\kappa_h<1$ is a constant. It is seen that $P_h(\boldsymbol{x})$ is smooth and lower bounded by zero, and the potential energy remains constant where $f_h(\boldsymbol{x})>0$.

Therefore, the overall potential energy is defined as the summation of $P_h(\boldsymbol{x})$ and $P_t(\boldsymbol{x})$ as:

$$P_{H-R}(\boldsymbol{x})=P_t(\boldsymbol{x})+P_h(\boldsymbol{x}). \tag{7}$$

where the notation of H–R denotes the scenario that human play an active role in the beginning and the robot only takes the control in the end. The fixed top contour of $P_{H-R}(\boldsymbol{x})$ corresponds to the high-order region $f_h(\boldsymbol{x})$, and its bottom part is the desired position $\boldsymbol{x}_d$.

Partial differentiating the potential energy function described by (7) with respect to $\boldsymbol{x}-\boldsymbol{x}_d$ yields:

$$\Big(\frac{\partial P_{H-R}(\boldsymbol{x})}{\partial(\boldsymbol{x}-\boldsymbol{x}_d)}\Big)^T=\Big(\frac{\partial P_t(\boldsymbol{x})}{\partial(\boldsymbol{x}-\boldsymbol{x}_d)}\Big)^T+\Big(\frac{\partial P_h(\boldsymbol{x})}{\partial(\boldsymbol{x}-\boldsymbol{x}_d)}\Big)^T\overset{\triangle}{=}\Delta\boldsymbol{\varepsilon}_{H-R}, \tag{8}$$

The vector $\Delta\boldsymbol{\varepsilon}_{H-R}$ denotes the region error. When the end effector is inside the human region where $f(\boldsymbol{x})>0$, $\Delta\boldsymbol{\varepsilon}_{R-H}=\mathbf{0}$, and human can take control to guide the end effector to enter the robot region. After the end effector enters the robot region where $f(\boldsymbol{x})\leq 0$, the region error $\Delta\boldsymbol{\varepsilon}_{H-R}$ is activated to drive the end effector to the desired position.

2) : Consider the second scenario in the previous subsection, the robot region is specified where $f(\boldsymbol{x})>0$ while the human region is specified where $f(\boldsymbol{x})\leq 0$. Therefore, the potential energy is specified as:

$$P_{R-H}(\boldsymbol{x})=\frac{k_x}{N}[max(0,f(\boldsymbol{x}))]^N, \tag{9}$$

where k_x is a positive constant, and the notation of R–H denotes the scenario that the robot is active in the beginning and human guide the robot to carry out manipulation tasks in the end. It is seen that $P_{R-H}(\boldsymbol{x})$ is smooth and lower bounded by zero. The bottom contour of the potential energy corresponds to the region function $f(\boldsymbol{x})$, and the potential energy naturally reduces to zero when the end effector transits from the robot region where $f(\boldsymbol{x})>0$ to the human region where $f(\boldsymbol{x})\leq 0$.

Partial differentiating the potential energy function described by (9) with respect to $\boldsymbol{x}-\boldsymbol{x}_d$ yields:

$$\left(\frac{\partial P_{R-H}(\boldsymbol{x})}{\partial(\boldsymbol{x}-\boldsymbol{x}_d)}\right)^T=k_x[max(0,f(\boldsymbol{x}))]^{N-1}\left(\frac{\partial f(\boldsymbol{x})}{\partial(\boldsymbol{x}-\boldsymbol{x}_d)}\right)^T\overset{\triangle}{=}\Delta\boldsymbol{\varepsilon}_{R-H}, \tag{10}$$

where $\Delta\boldsymbol{\varepsilon}_{R-H}$ denotes the region error. When the end effector is inside the robot region where $f(\boldsymbol{x})>0$, $\Delta\boldsymbol{\varepsilon}_{R-H}\neq\mathbf{0}$. When the end effector enters the human region where $f(\boldsymbol{x})\leq 0$, the region error $\Delta\boldsymbol{\varepsilon}_{R-H}$ automatically reduces to zero from equation (10). That is, the region error $\Delta\boldsymbol{\varepsilon}$ is employed to drive the end effector to transit from the robot region to the human region, and it reduces to zero after the end effector enters the human region.

IV. Adaptive Tracking Control for Human-Robot Co-manipulation

Based on the proposed human region and robot region, we can now proceed to develop the adaptive tracking control strategy for human-robot co-manipulation. The proposed controller plays an active role inside the robot region, and act passively inside the human region so as to allow the involvement of human control action.

First, a reference vector is proposed as:

$$\dot{\boldsymbol{q}}_r = \boldsymbol{J}^{+}(\boldsymbol{q})\dot{\boldsymbol{x}}_a - \alpha \boldsymbol{J}^{+}(\boldsymbol{q})\Delta\boldsymbol{\varepsilon}, \tag{11}$$

where $\boldsymbol{J}^{+}(\boldsymbol{q})$ is the pseudo-inverse matrix of $\boldsymbol{J}(\boldsymbol{q})$, α is a positive constant, the region error can be specified as either $\Delta\boldsymbol{\varepsilon} = \Delta\boldsymbol{\varepsilon}_{R-H}$ or $\Delta\boldsymbol{\varepsilon} = \Delta\boldsymbol{\varepsilon}_{H-R}$ according to the specific scenario of co-manipulation, and $\dot{\boldsymbol{x}}_a$ represents a reference vector defined as: $\dot{\boldsymbol{x}}_a = [\dot{x}_{d1}\frac{x_{b1}-x_1}{x_{b1}-x_{d1}}, \cdots, \dot{x}_{dp}\frac{x_{bp}-x_p}{x_{bp}-x_{dp}}]^T$ where $\dot{\boldsymbol{x}}_d = [\dot{x}_{d1}, \cdots, \dot{x}_{dp}]^T$ is the desired velocity. Next, the sliding vector is introduced as: $\boldsymbol{s} = \dot{\boldsymbol{q}} - \dot{\boldsymbol{q}}_r$. Using the sliding vector, the robot dynamics in equation (3) is written as:

$$\begin{aligned} &\boldsymbol{M}(\boldsymbol{q})\dot{\boldsymbol{s}} + [\tfrac{1}{2}\dot{\boldsymbol{M}}(\boldsymbol{q}) + \boldsymbol{S}(\boldsymbol{q}, \dot{\boldsymbol{q}})]\boldsymbol{s} + \\ &\boldsymbol{Y}_d(\boldsymbol{q}, \dot{\boldsymbol{q}}, \dot{\boldsymbol{q}}_r, \ddot{\boldsymbol{q}}_r)\boldsymbol{\theta}_d = \boldsymbol{\tau} + \boldsymbol{\tau}_e - \boldsymbol{d}. \end{aligned} \tag{12}$$

The human-guided manipulation controller is proposed as:

$$\boldsymbol{\tau} = -\boldsymbol{J}^T(\boldsymbol{q})\Delta\boldsymbol{\varepsilon} - \boldsymbol{K}_s\boldsymbol{s} + \boldsymbol{Y}_d(\boldsymbol{q}, \dot{\boldsymbol{q}}, \dot{\boldsymbol{q}}_r, \ddot{\boldsymbol{q}}_r)\hat{\boldsymbol{\theta}}_d, \tag{13}$$

where $\boldsymbol{K}_s$ is a positive definite matrix, and $\hat{\boldsymbol{\theta}}_d$ is a vector of estimated dynamic parameters which is updated by the following update law: $\dot{\hat{\boldsymbol{\theta}}}_d = -\boldsymbol{L}_d\boldsymbol{Y}_d^T(\boldsymbol{q}, \dot{\boldsymbol{q}}, \dot{\boldsymbol{q}}_r, \ddot{\boldsymbol{q}}_r)\boldsymbol{s}$ where $\boldsymbol{L}_d$ is a positive definite matrix. Note that $\Delta\boldsymbol{\varepsilon}$ is smooth with continuous partial derivatives, and thus the controller is also continuous without hard-switching.

When the end effector is inside the robot region, the region error $\Delta\boldsymbol{\varepsilon}$ is nonzero, and the proposed controller drives the robot to move to the desired position within the robot region or move from the robot region to the human region. When the end effector is inside the human region, the region error $\Delta\boldsymbol{\varepsilon}$ reduces to zero such that $\boldsymbol{\tau} = -\boldsymbol{K}_s\boldsymbol{s} + \boldsymbol{Y}_d(\boldsymbol{q}, \dot{\boldsymbol{q}}, \dot{\boldsymbol{q}}_r, \ddot{\boldsymbol{q}}_r)\hat{\boldsymbol{\theta}}_d$ where $\boldsymbol{s} = \dot{\boldsymbol{q}} - \boldsymbol{J}^{+}(\boldsymbol{q})\dot{\boldsymbol{x}}_a$. That is, only the velocity control term works, while the position control term $\boldsymbol{x} - \boldsymbol{x}_d$ is not included in the control input. Since human take control of the manipulator in the human region, the directional information towards the desired position $\boldsymbol{x}_d$ is provided by human, and the robot dynamics is also compensated by human.

Substituting equation (13) into equation (12), we have the following closed-loop equation:

$$\begin{aligned} &\boldsymbol{M}(\boldsymbol{q})\dot{\boldsymbol{s}} + [\tfrac{1}{2}\dot{\boldsymbol{M}}(\boldsymbol{q}) + \boldsymbol{S}(\boldsymbol{q}, \dot{\boldsymbol{q}})]\boldsymbol{s} + \boldsymbol{K}_s\boldsymbol{s} \\ &+ \boldsymbol{J}^T(\boldsymbol{q})\Delta\boldsymbol{\varepsilon} + \boldsymbol{Y}_d(\boldsymbol{q}, \dot{\boldsymbol{q}}, \dot{\boldsymbol{q}}_r, \ddot{\boldsymbol{q}}_r)\Delta\boldsymbol{\theta}_d = \boldsymbol{\tau}_e - \boldsymbol{d}, \end{aligned} \tag{14}$$

where $\Delta\boldsymbol{\theta}_d = \boldsymbol{\theta}_d - \hat{\boldsymbol{\theta}}_d$. A Lyapunov-like candidate V is then proposed as follows:

$$V = \tfrac{1}{2}\boldsymbol{s}^T\boldsymbol{M}(\boldsymbol{q})\boldsymbol{s} + P(\boldsymbol{x}) + \tfrac{1}{2}\Delta\boldsymbol{\theta}_d^T\boldsymbol{L}_d^{-1}\Delta\boldsymbol{\theta}_d, \tag{15}$$

where $P(\boldsymbol{x})$ denotes the potential energy function which is either specified as $P(\boldsymbol{x}) = P_{R-H}(\boldsymbol{x})$ or $P(\boldsymbol{x}) = P_{H-R}(\boldsymbol{x})$ according to the specific scenario of the co-manipulation.

Next, differentiating V with respect to time and substituting the sliding vector, the update law, and the closed-loop equation into it, we have:

$$\begin{aligned} \dot{V} = &-\boldsymbol{s}^T\boldsymbol{K}_s\boldsymbol{s} - \boldsymbol{s}^T[\boldsymbol{J}^T(\boldsymbol{q})\Delta\boldsymbol{\varepsilon} + \boldsymbol{Y}_d(\boldsymbol{q}, \dot{\boldsymbol{q}}, \dot{\boldsymbol{q}}_r, \ddot{\boldsymbol{q}}_r)\Delta\boldsymbol{\theta}_d] \\ &+ (\dot{\boldsymbol{x}} - \dot{\boldsymbol{x}}_a)^T\Delta\boldsymbol{\varepsilon} - \dot{\hat{\boldsymbol{\theta}}}_d^T\boldsymbol{L}_d^{-1}\Delta\boldsymbol{\theta}_d + \boldsymbol{s}^T(\boldsymbol{\tau}_e - \boldsymbol{d}) \\ = &-\boldsymbol{s}^T\boldsymbol{K}_s\boldsymbol{s} - \alpha\Delta\boldsymbol{\varepsilon}^T\Delta\boldsymbol{\varepsilon} + \boldsymbol{s}^T(\boldsymbol{\tau}_e - \boldsymbol{d}). \end{aligned} \tag{16}$$

Equation (16) can rewritten as:

$$\dot{V} = -W + \boldsymbol{s}^T(\boldsymbol{\tau}_e - \boldsymbol{d}), \tag{17}$$

where $W = \boldsymbol{s}^T\boldsymbol{K}_s\boldsymbol{s} + \alpha\Delta\boldsymbol{\varepsilon}^T\Delta\boldsymbol{\varepsilon}$. Integrating equation (17) over $[0, t]$ yields: $\int_0^t \boldsymbol{s}^T(\varsigma)[\boldsymbol{\tau}_e(\varsigma) - \boldsymbol{d}(\varsigma)]\mathrm{d}\varsigma = V(t) - V(0) + \int_0^t W(\varsigma)\mathrm{d}\varsigma$. Since both V and W are non-negative, we have:

$$\int_0^t \boldsymbol{s}^T(\varsigma)[\boldsymbol{\tau}_e(\varsigma) - \boldsymbol{d}(\varsigma)]\mathrm{d}\varsigma \geq -V(0). \tag{18}$$

The above equation (18) demonstrates the passivity of the dynamics between the input $\boldsymbol{\tau}_e - \boldsymbol{d}$ and output $\boldsymbol{s}$. We are now ready to state the following theorem:

Theorem 1: *The sliding vector $\boldsymbol{s}$ is bounded if the external torque $\boldsymbol{\tau}_e$ exerted by human and the unmodeled torque $\boldsymbol{d}$ are bounded, and $\boldsymbol{K}_s$ is chosen sufficiently large so that:*

$$\tfrac{1}{\gamma^2} \overset{\triangle}{=} 2\lambda_{min}[\boldsymbol{K}_s] - 1 > 0, \tag{19}$$

where $\gamma > 0$, and $\lambda_{min}[\bullet]$ denotes the minimum eigenvalue.

Proof: Note that

$$\begin{aligned} \int_0^t \boldsymbol{s}^T(\varsigma)[\boldsymbol{\tau}_e(\varsigma) - \boldsymbol{d}(\varsigma)]\mathrm{d}\varsigma &\leq \tfrac{1}{2}\int_0^t ||\boldsymbol{s}(\varsigma)||^2\mathrm{d}\varsigma \\ &+ \tfrac{1}{2}\int_0^t ||\boldsymbol{\tau}_e(\varsigma) - \boldsymbol{d}(\varsigma)||^2\mathrm{d}\varsigma. \end{aligned} \tag{20}$$

From equations (17) and (20), we have:

$$\begin{aligned} &-V(0) + \int_0^t W(\varsigma)\mathrm{d}\varsigma \\ &\leq \tfrac{1}{2}\int_0^t ||\boldsymbol{s}(\varsigma)||^2\mathrm{d}\varsigma + \tfrac{1}{2}\int_0^t ||\boldsymbol{\tau}_e(\varsigma) - \boldsymbol{d}(\varsigma)||^2\mathrm{d}\varsigma. \end{aligned} \tag{21}$$

Since $V > 0$, substituting W into equation (21) yields:

$$\begin{aligned} &(2\lambda_{min}[\boldsymbol{K}_s] - 1)\int_0^t ||\boldsymbol{s}(\varsigma)||^2\mathrm{d}\varsigma + 2\alpha\int_0^t ||\Delta\boldsymbol{\varepsilon}(\varsigma)||^2\mathrm{d}\varsigma \\ &\leq \int_0^t ||\boldsymbol{\tau}_e(\varsigma) - \boldsymbol{d}(\varsigma)||^2\mathrm{d}\varsigma + 2V(0). \end{aligned} \tag{22}$$

Next, using equation (19), we have:

$$\int_0^t ||\boldsymbol{s}(\varsigma)||^2\mathrm{d}\varsigma \leq \gamma^2\int_0^t ||\boldsymbol{\tau}_e(\varsigma) - \boldsymbol{d}(\varsigma)||^2\mathrm{d}\varsigma + k(0), \tag{23}$$

where $k(0) = 2\gamma^2 V(0)$. Therefore, the sliding vector $\boldsymbol{s}$ is bounded since the torque $\boldsymbol{\tau}_e$ exerted by human and the unmodeled torque $\boldsymbol{d}$ are bounded. $\triangle\triangle\triangle$

It is well known that human are able to adapt to unknown forces and act intelligently without accurate knowledge of the environment. Next, we consider the case where the human force is able to learn or adapt to the unmodeled external torque such that $\boldsymbol{\tau}_e \to \boldsymbol{d}$ as $t \to \infty$. The following theorem states the effects of human adaption on the overall system:

Theorem 2: *The closed-loop system described by (14) gives rise to the convergence of the region error, if the condition described by (19) is satisfied and human are able to adapt and reach for the desired target.*

Proof: In the first scenario that human play the active role in the beginning, if the end effector is guided by human to move from the human region to the desired robot region, the desired target is reached. In the second scenario that human take control in the ending stage, the desired target is reached if the end effector is guided to move to the desired position. When the end effector is located at the robot region in either scenario, the proposed controller (13) is activated which leads to the closed-loop equation (14).

Next, equation (23) is obtained if the condition described by (19) is satisfied. Equation (23) indicates that $\boldsymbol{s}$ is bounded since $\boldsymbol{\tau}_e - \boldsymbol{d}$ is bounded. From equation (17), we have:

$$V(t)+\int_0^t W(\varsigma)\mathrm{d}\varsigma=\int_0^t \boldsymbol{s}^T(\varsigma)[\boldsymbol{\tau}_e(\varsigma)-\boldsymbol{d}(\varsigma)]\mathrm{d}\varsigma+V(0). \quad (24)$$

since $\boldsymbol{s}$ is bounded and $\boldsymbol{\tau}_e - \boldsymbol{d} \to \mathbf{0}$, $\int_0^t \boldsymbol{s}^T(\varsigma)[\boldsymbol{\tau}_e(\varsigma)-\boldsymbol{d}(\varsigma)]\mathrm{d}\varsigma$ is bounded, and hence both V and $\int_0^t W(\varsigma)\mathrm{d}\varsigma$ are bounded. Since V is bounded, $\boldsymbol{s}$, $\Delta\boldsymbol{\theta}_d$, $P(\boldsymbol{x})$ are bounded. The boundedness of $P(\boldsymbol{x})$ ensures the boundedness of $f(\boldsymbol{x})$. Since the region function is bounded, $\boldsymbol{x}$ is bounded if the desired position $\boldsymbol{x}_d$ is bounded. Therefore, $\Delta\boldsymbol{\varepsilon}$ is bounded. Since $\Delta\boldsymbol{\varepsilon}$ is bounded, $\dot{\boldsymbol{q}}_r$ is bounded, and $\dot{\boldsymbol{q}}$ is bounded because $\boldsymbol{s}$ is bounded. The boundedness of $\dot{\boldsymbol{q}}$ guarantees the boundedness of $\dot{\boldsymbol{x}}$ since $\boldsymbol{J}(\boldsymbol{q})$ are trigonometric functions of $\boldsymbol{q}$. Therefore, $\Delta\dot{\boldsymbol{\varepsilon}}$ is bounded, and $\Delta\boldsymbol{\varepsilon}$ is uniformly continuous. Since $\int_0^t W(\varsigma)\mathrm{d}\varsigma = \int_0^t(\boldsymbol{s}^T\boldsymbol{K}_s\boldsymbol{s} + \alpha\Delta\boldsymbol{\varepsilon}^T\Delta\boldsymbol{\varepsilon})\mathrm{d}\varsigma$ is bounded, it is easy to verify that $\Delta\boldsymbol{\varepsilon} \in L_2(0,\infty)$. Therefore, it follows from [27], [29], [30] that $\Delta\boldsymbol{\varepsilon} \to \mathbf{0}$, and $\Delta\boldsymbol{\varepsilon} = \mathbf{0}$ implies that the position of the end effector converges to the desired position after the end effector enters the robot region in the first scenario of $H-R$, or the end effector is controlled to move from the robot region to the human region in the second scenario of R–H. △△△

V. Experiment

The proposed control scheme was implemented on the first two joints of a SONY SRX-4CH industrial manipulator.

A. Human-Guided Visual Tracking

In the first experiment, a PSD camera is employed to measure the position of the end effector in image space (in the unit of voltage [31]). While the vision ensures the high-accurate positioning of the end effector, the vision is not available if the end effector starts from a large initial position, and the robot does not have any visual information of the environment that is outside the view.

To solve the problem, the environment of the workspace that is outside the view of the camera is defined as the human region. Human guide the end effector to transit from the human region to the robot region. After the end effector enters the robot region, the visual feedback is activated and used to drive the end effector to the desired position. The region function in equation (4) is specified as:

$$f(\boldsymbol{x}_I)=\frac{(x_{I1}-x_{d1})^2}{(x_{b1}-x_{d1})^2}+\frac{(x_{I2}-x_{d2})^2}{(x_{b2}-x_{d2})^2}-1\leq 0, \quad (25)$$

and the high-order region that matches the FOV is specified as: $f_h(\boldsymbol{x}_I)=\frac{(x_{I1}-x_{d1})^{20}}{(x_{b1}-x_{d1})^{20}}+\frac{(x_{I2}-x_{d2})^{20}}{(x_{b2}-x_{d2})^{20}}-1\leq 0$, where $x_{b1}=-3$ volt if $x_{I1}\leq x_{d1}$ else x_{b1}=3 volt; x_{b2}=−3 volt if $x_{I2}\leq x_{d2}$ else x_{b2}=3 volt, and the desired position $\boldsymbol{x}_d$ is specified as a circle as: $x_{d1} = -1+\sin(0.4t)$ volt, and $x_{d2} = 1+\cos(0.4t)$ volt. Human take control of the manipulator where $f_h(\boldsymbol{x}_I)>0$, and the robot becomes active where $f_h(\boldsymbol{x}_I)\leq 0$.

The control parameters in equation (13) were set as: α=50, k_t=3.5, k_h=3.5, κ=0.7, $\boldsymbol{K}_s$=$diag\{0.0001, 0.0001\}$, $\boldsymbol{L}_d$=$diag\{0.0001, 0.0001\}$, the region error is specified as $\Delta\boldsymbol{\varepsilon}$=$\Delta\boldsymbol{\varepsilon}_{H-R}$ since human play an active role in the beginning and the robot only takes the control in the end. The experimental results are shown in Fig. 3. As seen from Fig. 3(a) and Fig. 3(b), the end effector transits from the human region to the robot region and converges to the desired position within the robot region. As seen from Fig. 3(c), the tracking errors reduce to zero after the end effector enters the robot region.

B. Human-Guided Setpoint Control

In the second experiment, the robot end effector is controlled to move to a neighborhood around the desired position by using the Cartesian-space feedback only. A Cartesian-space region is formulated to enclose the desired position, where the robot region is specified outside the Cartesian-space region and the human region is specified inside the Cartesian-space region. After the end-effector transits from the robot region to the human region, the robot becomes passive, and human identify the desired position and guide the end effector to move to the desired position.

The region function in equation (4) is specified as:

$$f(\boldsymbol{r})=\frac{(r_1-r_{d1})^2}{0.1^2}+\frac{(r_2-r_{d2})^2}{0.1^2}-1\leq 0, \quad (26)$$

and the desired position $\boldsymbol{r}_d$ is specified as a setpoint as: $r_{d1} = -0.4$ m, and $r_{d2} = 0.2$ m. The robot plays a more active role where $f(\boldsymbol{r})>0$, and the human control action is fully activated where $f(\boldsymbol{r})\leq 0$. The control parameters in equation (13) were set as: $\alpha = 10$, $k_x = 2$, $\boldsymbol{K}_s = diag\{0.05,\ 0.05\}$, $\boldsymbol{L}_d$=$diag\{0.0001, 0.0001\}$, and the region error is specified as $\Delta\boldsymbol{\varepsilon}=\Delta\boldsymbol{\varepsilon}_{R-H}$ since the robot is active in the beginning and human guide the robot to carry out manipulation tasks in the end. The experimental results are shown in Fig. 4. As seen from Fig. 4(a), the end effector first moves from the robot region to the human region, and it is then guided by human to the desired position within the human region. As seen from Fig. 4(b), the position errors converge to small bounds at steady state.

VI. Conclusion

In this paper, a human-guided manipulation problem has been formulated and solved. The proposed method allows us to take advantages of both the human knowledge and the robot's ability in a stable manner. The combination of the human and robot co-manipulation is illustrated in various scenarios, and an adaptive tracking controller is then developed for the human-guided robotic manipulation. It has been shown that the stability of the closed-loop system that involves human-robot interaction can be ensured. Experimental results have been presented to illustrate the performance of the proposed method in different scenarios of human-robot co-manipulation. We believe that such formulation would bridge the gap between traditional robot control and physical human-robot interaction control.

References

[1] H. I. Krebs, N. Hogan, M. L. Aisen, and B. T. Volpe, "Robot-aided neurorehabilitation," *IEEE Trans. Rehabilitation Eng.*, Vol. 6, No. 1, pp. 75-87, 1998.

[2] H. I. Krebs, J. J. Palazzolo, L. Dipietro, M. Ferraro, J. Krol, K. Rannekleiv, B. T. Volpe, and N. Hogan, "Rehabilitation robotics: performancebased progressive robot-assisted therapy," *Autonomous Robots*, Vol. 15, No. 1, pp. 7-20, 2003.

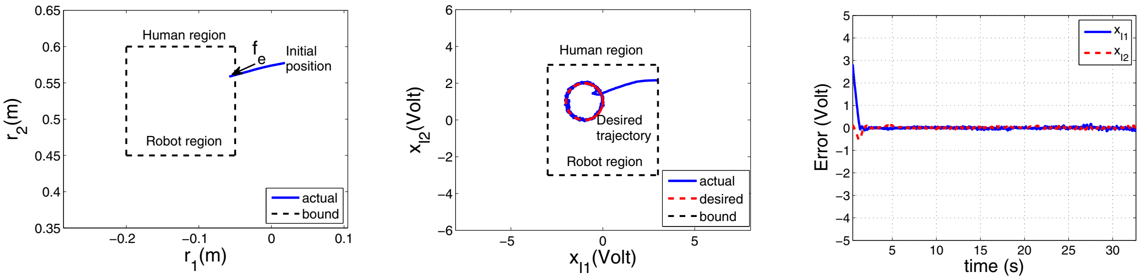

(a) Path of end effector in Cartesian space (b) Path of end effector in image space (c) Tracking errors

Fig. 3. Experiment 1: Human exert an external force f_e on the end effector and guide it to transit from the human region to the robot region. After the end effector enters the robot region, the vision-based control is activated and drives the end effector to the desired position.

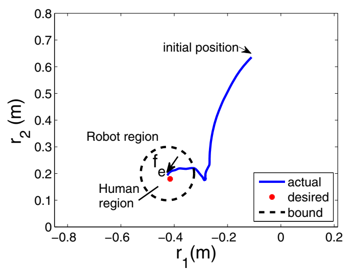

(a) Path of end effector in Cartesian space

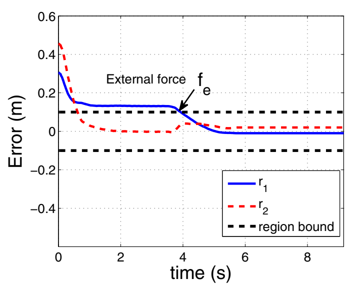

(b) Position errors

Fig. 4. Experiment 2: The end effector is controlled to move from the robot region to the human region with Cartesian-space feedback only, and then human exert an external force f_e on the end effector and guide it to move to the desired position after it enters the human region.

[3] H. I. Krebs, B. Volpe, D. Williams, J. Celestino, S. Charles, D. Lynch, and N. Hogan, "Robot-aided neurorehabilitation: a robot for wrist rehabilittion," *IEEE Trans. Neural Syst. Rehabilitation Eng.*, Vol. 15, No. 3, pp. 327-335, 2007.

[4] H. Kazerooni, J. L. Racine, L. Huang, and R. Steger, "On the control of the Berkeley Lower Extremity Exoskeleton (BLEEX)," *IEEE Int. Conf. Robotics Automat.*, pp. 4353-4360, 2005.

[5] A. M. Dollar, and H. Herr, "Lower extremity exoskeletons and active orthoses: challenges and Stage-of-the Art," *IEEE Trans. Robotics*, Vol. 24, No. 1, pp. 144-158, 2008.

[6] M. Takegaki, and S. Arimoto, "A new feedback method for dynamic control of manipulators," *ASME J. Dynamic Syst. Meas. Control*, Vol. 102, pp. 119-125, 1981.

[7] J. J. E. Slotine, and W. Li, "On the adaptive control of robot manipulators," *Int. J. Robotics Res.*, No. 6, pp. 49-59, 1987.

[8] G. Niemeyer, and J. J. E. Slotine, "Performance in adaptive manipulator control," *Int. J. Robotics Res.*, 10(2), 149-161, 1991.

[9] C. C. Cheah, M. Hirano, S. Kawamura and S. Arimoto, "Approximate Jacobian control for robots with uncertain kinematics and dynamics," *IEEE Trans. Robotics Automat.*, 19(4), 692-702, 2003.

[10] W. E. Dixon, "Adaptive regulation of amplitude limited robot manipulators with uncertain kinematics and dynamics," *IEEE Trans. Automatic Control*, Vol. 52, No. 3, pp. 488-493, 2007.

[11] C. C. Cheah, C. Liu, and J. J. E. Slotine, "Adaptive tracking controls for robots with unknown kinematics and dynamic properties," *Int. J. Robotics Res.*, Vol. 25, No. 3, pp. 283-296, 2006.

[12] C. C. Cheah, D. Q. Wang, and Y. C. Sun, "Region-reaching control of robots," *IEEE Trans. Robotics*, 23(6), 1260-1264, 2007.

[13] X. Li, and C. C. Cheah, "Global task-space adaptive control of robot," *Automatica*, Vol. 49, No. 1, pp. 58-69, 2013.

[14] S. Haddadin, A. Albu-Schaffer, A. De Luca, and G. Hirzinger, "Collision detection and reaction: a contribution to safe physical human-robot interaction," *IEEE Int. Conf. Robotics Automat.*, pp. 3356-3363, 2008.

[15] Y. Yamada, Y. Hirasawa, S. Huang, Y. Umetani, and K. Suita, "Human robot contact in the safeguarding space," *IEEE/ASME Trans. Mechatronics*, Vol. 2, No. 4, pp. 230-236, 1997.

[16] G. Palli, C. Melchiorri, and A. De Luca, "On the feedback linearization of robots with variable joint stiffness," *IEEE Int. Conf. Robotics Automat.*, pp. 1753-1759, 2008.

[17] A. De Luca, F. Flacco, A. Bicchi, and R. Schiavi, "Nonlinear decoupled motion-stiffness control and collision detection/reaction for the VSA-II variable stiffenss device," *IEEE Int. Conf. Robotics Automat.*, pp. 5487-5494, 2009.

[18] A. Bicchi, and G. Tonietti, "Fast and "soft-arm" tactics [robot arm design]," *IEEE Robotics and Automation Magazine*, Vol. 11. No. 2, pp. 22-33, 2004.

[19] E. D. Fasse, and N. Hogan, "Control of physical contact and dynamic interaction," *Int. Symp. Robotics Res.*, 1995.

[20] N. Hogan, "Impedance control: an approach to manipulation," *ASME J. Dynamic Syst. Meas. Control*, Vol. 107, pp. 1-24, 1985.

[21] N. Hogan, and S. P. Buerger, "Impedance and interaction control," *Robotics and Automation Handbook*, CRC Press, 2001.

[22] C. C. Cheah, and D. Wang, "Learning impedance control for robotic manipulators," *IEEE Trans. Robotics Automat.*, Vol. 14, No. 3, pp. 452-465, 1998.

[23] J. A. Saglia, N. G. Tsagarakis, J. S. Dai, and D. G. Caldwell, "Control strategies for ankle rehabilitation using a high performance ankle exerciser," *IEEE Int. Conf. Robotics Automat.*, pp. 2221-2227, 2010.

[24] F. Petit, and A. Albu-Schaffer, "Cartesian impedance control for A variable stiffness robot arm," *IEEE/RSJ Int. Conf. Intelligent Robots Systems*, pp. 4180-4186, 2011.

[25] E. Gribovskaya, A. Kheddar, and A. Billard, "Motion learning and adaptive impedance for robot control during physical interaction with humans," *IEEE Int. Conf. Robotics Automat.*, pp. 4326-4332, 2011.

[26] J. Zhang, C. C. Cheah, and S. H. Collins, "Stable human-robot interaction control for upper-limb rehabilitation robotics," *IEEE Int. Conf. Robotics Automat.*, pp. 2201-2206, 2013.

[27] S. Arimoto, *Control Theory of Non-Linear Mechanical Systems*. Oxford University Press, 1996.

[28] F. L. Lewis, C. T. Abdallah, and D. M. Dawson, *Control of Robot End-effectors*. New York: Macmillan Publishing Company, 1993.

[29] M. W. Spong, and M. Vidyasagar, *Robot Dynamics and Control*. New York: John Wiley & Sons, 1989.

[30] J. J. E. Slotine, and W. Li, *Applied Nonlinear Control*. Englewood Cliffs, New Jersy: Prentice Hall, 1991.

[31] http://www.jr3.com/index.html